JCAMECH
Vol. 46, No. 2, July 2015, pp 133- 151

Dynamic responses of poroelastic beams with attached mass-spring systems and time-dependent, non-ideal supports subjected to moving loads: An analytical approach

S. Fallahzadeh R.[1] and M. Shariyat[2*]

1. M.Sc., Faculty of Mechanical Engineering, K.N. Toosi University of Technology, Tehran, Iran
2. Professor, Faculty of Mechanical Engineering, K.N. Toosi University of Technology, Tehran, Iran

Received 16 December 2014; Accepted 9 January 2015

Abstract
The present study is the first to analyze the dynamic response of a poroelastic beam subjected to a moving force. Moreover, the influences of attached mass-spring systems and non-ideal supports (with local movements in the supporting points or base due to the presence of factors such as gaps, unbalanced masses, and friction or seismic excitations) on the responses were investigated. Non-ideal support experiences time-dependent deflection and moment. To evaluate the effects of both the theory type and the material properties, three models were investigated for the beam with mass-spring attachment and non-ideal supports: i) elastic Euler-Bernoulli-type beam, ii) elastic Timoshenko-type beam, and iii) poroelastic beam. The governing-coupled PDE equations of the forced vibration of the saturated poroelastic beam were analytically solved via Laplace and finite Fourier transforms. The effects of various parameters on the responses were investigated comprehensively and illustrated graphically. The poroelastic nature of the material properties was found to attenuate the vibration amplitude, and it is assumed that the attached mass can considerably affect the vibration pattern.

Keywords: *Poroelastic beam, Dynamic response, Finite Fourier transform, Laplace transform, Non-ideal support, Attached mass-spring system.*

1. Introduction

Investigation of the forced vibration behavior of structures carrying mass-spring systems is an important issue in several engineering structures, including the automotive, aerospace, marine, and civil structures. The control and measurement instruments attached to a control board and the navigation instrumentations as well as the passengers and sprung masses (e.g., the differential) of a vehicle may be regarded as an attached mass-spring systems [1,2]. Moreover, it has been experimentally verified that a person or a crowd on a bridge or narrow plate-type

[*] Corresponding Author: E-mail: m_shariyat@yahoo.com and shariyat@kntu.ac.ir

structure may be regarded as an attached mass-spring or mass-spring-damper system when considering the interaction between the human and the structure [3]. The attached mass-spring system may be deliberately included into the structure to serve as a dynamic vibration absorber [4]. On the other hand, concrete or wooden beams may be regarded as poroelastic beams. Therefore, some combinations, such as the vehicle-bridge combination, may be modeled by a poroelastic beam with attached mass-spring system that may be exposed to the excitation of faster moving vehicles.

Numerous papers are available on isotropic [5], functionally graded, and viscoelastic [6] beams with moving loads provided by either moving masses [7] or concentrated loads [8-10], mainly based on the Euler-Bernoulli beam theory. Vibration of a transversely graded simply supported beam due to a moving load was investigated by Şimşek [11] by employing the Timoshenko beam theory. Wang and Chen [12] studied the effects of the acceleration of a moving mass on the beam responses. On the other hand, vibration of continuous systems with mass attachments has been the topic of some recent investigations. Turhan [13] analyzed the fundamental frequencies of an Euler-Bernoulli beam with an attached point mass. Chiba and Sugimoto [14] considered the vibration characteristics of a cantilever plate with a mass-spring system attached to it by using the Rayleigh-Ritz method.

Several structural components such as those used in bioengineering and bioscience (e.g., bones), civil engineering (e.g., wooden piles), and ventilation facilities exhibit poroelastic or saturated poroelastic behaviors. In several applications, these elements may be modeled on the basis of the Euler-Bernoulli or Timoshenko beam theories in conjunction with the Biot theory of the saturated porous media. Zhang and Cowin [15] studied steady-state vibrations of a saturated poroelastic isotropic beam under cyclic loadings. Based on the three-dimensional Biot model, Wang et al. [16] presented a linear analytical solution for the steady and transient pure bending responses of a compressible saturated poroelastic eam. Li et al. [17] presented a geometrically non-linear, but constitutively linear formulation for large deflection of the fluid-saturated poroelastic beams that were permeable in the axial direction and impermeable in the transverse direction as per the Euler-Bernoulli beam theory.

Often, under several conditions, the fluid or solid phases can be assumed to be incompressible from the microscopic perspective. While the Biot theory [18,19] has been commonly employed for the saturated poroelastic media, the theory of porous media [20] and the theory of hybrid mixture [21] have also been successfully employed in several fields of study such as soil dynamics, geophysics, and biomechanics. Using the Biot theory, Yang and Wang [22] analyzed the dynamic behavior of a saturated poroelastic cantilever beam subjected to a harmonic-end load by the finite element method. Yang and Wen [23] performed the dynamic analysis of a saturated poroelastic Timoshenko cantilever beam with an impermeable fixed-end and a permeable free-end that were subjected to a step-end load by considering the movement of the pore fluid in the axial direction only. The governing equations were solved by the Laplace transform. Based on the theory of porous media, Yi et al. [24] investigated the quasi-static and dynamical bending of a cantilever poroelastic beam subjected to a step-end load.

Few investigations have been accomplished on the dynamical and quasi-static behavior of the hydro-mechanical coupling of various saturated poroelastic structures. On the basis of the Biot model, Niskos et al. [25] investigated the bending deformations of poroelastic plates. Busse et al. [26] presented a dynamical mathematical model for the Mindlin plates. Assuming the axial movement of the pore fluid only, the natural frequencies and attenuations of the free and forced vibrations of the simply supported saturated poroelastic Timoshenko beams subject to step loads were investigated by Yang [27].

Specifications of the boundary and edge conditions significantly affect the dynamic responses and the frequencies of the resulting vibrations. For example, a beam simply supported at its both ends may be immovable and moment-free at both ends. However, due to manufacturing tolerances, the hole and pin (pivot) assembly may have a small gap and/or friction at the support, which may introduce small local relative displacements and/or moments. The same is true for a beam that is supported by bearings at its ends, except that the situation is more complex as, in this case, the resulting deflections and moments may be time-dependent. This situation occurs frequently in the automotive, aerospace, and civil engineering assemblies (in the latter, such a situation may occur during an earthquake). Pakdemirli and Boyaci investigated this effect by using the perturbation techniques [28]. Later, they investigated the effects of non-ideal support on non-linear vibration of a beam [29]. The effects of the non-ideal, simply supported boundary conditions on the vibration of rectangular isotropic plates were considered by Aydogdu and Ece [30]. Malekzadeh et al. [31] investigated the effects of non-ideal boundary condition on the vibrations of laminated plates based on elastic foundations. Boyaci [32] considered a simply supported, damped, Euler-Bernoulli beam with immovable non-ideal end conditions that allow small deflections and moments and they found an approximate analytical solution by using the multiple-scales perturbation technique. Eigoli and Ahmadian [33] investigated the influences of non-ideal boundary conditions on the nonlinear vibration of damped Euler–Bernoulli beams subjected to harmonic loads in the form of small deflections and/or moments at the supports of the beam by using the iteration perturbation method.

Considering that there is no published literature on the dynamic analysis of poroelastic beams with moving loads, especially for beams with non-ideal supports and attached mass-spring systems, we undertook this task in the present research. The end support of the beam has a time-dependent, non-ideality that is unprecedented in the field. The governing equations are solved analytically by using Laplace and finite Fourier transforms. Results of three different models have been compared through a sensitivity analysis for beams with attached spring-mass system: i) elastic Euler-Bernoulli, ii) elastic Timoshenko, and iii) poroelastic beams. In this regard, the effects of various parameters, such as the non-ideality of the right support, amount of the attached mass, and poroelastic material properties, have been investigated and discussed comprehensively in the Results section.

2. The governing equations of the problem

2.1. The elastic Euler-Bernoulli beam

The governing equation of vibration of an Euler-Bernoulli beam subjected to axial and transverse loads is given below [35]:

$$D\frac{\partial^4 w}{\partial x^4}+\rho A\frac{\partial^2 w}{\partial t^2}-P\frac{\partial^2 w}{\partial x^2}=f\left(x,t\right) \tag{1}$$

where, $D = EI$ is the reduced flexural rigidity of the beam and E, I, $w(x,t)$, ρ, A, and P are the elasticity modulus, inertia moment of the cross-section, transverse deflection of the beam, mass density, cross-section, and axial load of the beam, respectively. The beam with attached a mass-spring system, moving load, and non-ideal support are shown in Figure 1. For this beam, the distributed transverse load, $f(x,t)$, may be expressed as follows:

$$\begin{aligned}&f\left(x,t\right)=\left[m\,g-m\,\ddot{y}\left(t\right)\right]\delta\left(x-x_o\right)+\\&f_0\,\delta(x-x_1);\qquad x_1=Vt\end{aligned} \tag{2}$$

where, g, $y(t)$, and L are the gravity acceleration, absolute vertical position of the mass relative to the static equilibrium point, and length of the beam, while $\delta(x\text{-}x_0)$ is the Dirac delta function. Rewriting of Equation (1) gives the following equation:

$$\begin{aligned}&E\,I\,\frac{\partial^4 w}{\partial x^4}+\rho A\frac{\partial^2 w}{\partial t^2}-P\frac{\partial^2 w}{\partial x^2}=\\&m\left[\,g-\ddot{y}\left(t\right)\right]\delta\left(x-x_o\right)+\\&f_0\,\delta(x-x_1);\;x_1=Vt\quad t>0\end{aligned} \tag{3}$$

where $x_0\in(0,L)$ and V are the uniform velocity of the moving concentrated load. On the other hand, the governing equation of motion of the attached mass is as follows:

$$m\ddot{y}+k\,y=k\,w(x_0,t) \tag{4}$$

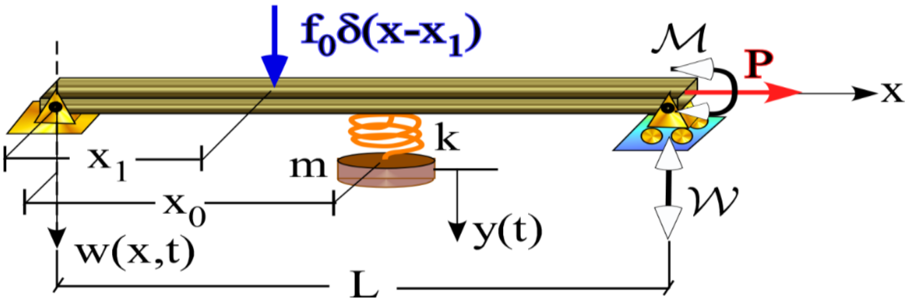

Fig. 1. A poroelastic beam with an attached mass-spring system and a non-ideal support

The following mathematical description was considered for the ideal and non-ideal simply supported boundary conditions of the beam:

$$w(0,t)=0,\quad \frac{\partial^2 w(0,t)}{\partial^2 x}=0,$$
$$w(L,t)=\mathcal{W}=\varepsilon_1 f_1(t),\quad \frac{\partial^2 w(L,t)}{\partial x^2}=\varepsilon_2 f_2(t) \tag{5}$$

where, ε_1 and ε_2 are the amplitudes of the time-dependent deflection and normalized moment acting on the non-ideal, right-hand support of the beam due to factors such as movements of the base of the support, presence of a gap, friction between the pin and hole of the supporting pivot, and presence of unbalanced masses. Therefore, these types of excitations may be produced by some kind of bearings as explained previously. These parameters serve as perturbation parameters of the non-ideal boundary conditions. The initial conditions of the beam were as follows:

$$y(0)=y_0,\qquad \dot{y}(0)=0 \tag{6}$$

$$w(x,0)=g_1(x);\qquad \frac{\partial w(x,0)}{\partial t}=g_2(x) \tag{7}$$

To cover the common practical situations, the support excitations are assumed to be harmonic, e.g., $f_1(t)=f_2(t)=\sin(bt)$, to determine the analytical solutions of the problem.

2.2. The elastic Timoshenko-type beam

Timoshenko bam theory may be adopted to incorporate the effects of shear deformations in the elastic beam. The relevant governing equation of motion of the beam shown in Figure 1 has the following form:

$$EI\frac{\partial^4 w}{\partial x^4}-P\frac{\partial^2 w}{\partial x^2}+\rho A\frac{\partial^2 w}{\partial t^2}-\rho I\left(1+\frac{E}{\kappa G}\right)\frac{\partial^4 w}{\partial x^2\partial t^2}+\frac{\rho^2 I}{\kappa G}\frac{\partial^4 w}{\partial t^4}=-\frac{EI}{\kappa AG}\frac{\partial^2 f}{\partial x^2}+\frac{\rho I}{\kappa AG}\frac{\partial^2 f}{\partial t^2}+f\qquad t>0 \tag{8}$$

where G is shear modulus of the material of the beam and   is the shear correction factor. As in the former case, the distributed transverse force may be described by Equation (2). Therefore, the right hand side of Equation (8) becomes as given below:

$$-\frac{EI}{\kappa AG}\frac{\partial^2 f}{\partial x^2}+\frac{\rho I}{\kappa AG}\frac{\partial^2 f}{\partial t^2}+f=-\frac{EI}{\kappa AG}\left[m(g-\ddot{y})\delta^{(2)}(x-x_0)+f_0\delta^{(2)}(x-Vt)\right]+\frac{\rho I}{\kappa AG}\left[-my^{(4)}\delta(x-x_0)+V^2 f_0\delta^{(2)}(x-Vt)\right]+m(g-\ddot{y})\delta(x-x_0)+f_0\delta(x-Vt);\ x_0,x_1\in(0,L) \tag{9}$$

in which $\delta^{(2)}(x-x_0)$ is the second derivative of the Dirac delta function with the following definition:

$$\int_{-\infty}^{\infty}\delta^{(2)}(x-x_0)\,f(x)\,dx=f''(x_0) \tag{10}$$

The governing Equation of motion of the attached mass is identical to Equation (4). The boundary conditions of the simply supported beam with ideal and non-ideal supports shown in Figure 1 are as follows:

$$w(0,t)=0,\qquad \frac{\partial\varphi(0,t)}{\partial x}=0 \tag{11}$$

$$w(L,t)=\varepsilon_1\sin(bt),\qquad \frac{\partial\varphi(L,t)}{\partial x}=\varepsilon_2\sin(bt) \tag{12}$$

in which, according to the Timoshenko beam theory, the rotation φ may be related to the lateral deflection as follows:

$$\frac{\partial\varphi}{\partial x}=\frac{\partial^2 w}{\partial x^2}-\frac{\rho}{\kappa G}\frac{\partial^2 w}{\partial t^2}+\frac{f}{\kappa AG} \qquad (13)$$

Such that $f(0,t)=f(L,t)=0$ and the boundary conditions of Equations (11) and (12) become:

$$w(0,t)=0,\quad \frac{\partial\varphi(0,t)}{\partial x}=\frac{\partial^2 w(0,t)}{\partial x^2}-\frac{\rho}{\kappa G}\frac{\partial^2 w(0,t)}{\partial t^2}=0 \qquad (14)$$

$$w(L,t)=\varepsilon_1\sin(bt),\quad \frac{\partial\varphi(L,t)}{\partial x}=\frac{\partial^2 w(L,t)}{\partial x^2}-\frac{\rho}{\kappa G}\frac{\partial^2 w(L,t)}{\partial t^2}=\varepsilon_2\sin(bt) \qquad (15)$$

Since $w(0,t)$ is constant with respect to time, its time derivatives become zero. Hence, $\frac{\partial^2 w(0,t)}{\partial t^2}=0$, and $w(L,t)=\varepsilon_1\sin(bt)$, so that $\frac{\partial^2 w(L,t)}{\partial t^2}=-\varepsilon_1 b^2\sin(bt)$. Therefore

$$w(0,t)=0,\quad \frac{\partial^2 w(0,t)}{\partial x^2}=0 \qquad (16)$$

$$w(L,t)=\varepsilon_1\sin(bt),\quad \frac{\partial^2 w(L,t)}{\partial x^2}=\left(\varepsilon_2-\frac{\rho b^2}{\kappa G}\varepsilon_1\right)\sin(bt) \qquad (17)$$

The initial conditions are follows:

$$y(0)=y_0,\quad \dot y(0)=0,\quad \ddot y(0)=0,\quad \dddot y(0)=0, \qquad (18)$$

$$w(x,0)=g_1(x),\quad \frac{\partial w(x,0)}{\partial t}=g_2(x),\quad \frac{\partial^2 w(x,0)}{\partial t^2}=0,\quad \frac{\partial^3 w(x,0)}{\partial t^3}=0. \qquad (19)$$

2.3. The poroelastic beam

Using Biot theory of the saturated porous media and neglecting the effects of the axial force and the axial displacements [19], the governing equations of vibration of the poroelastic Euler-Bernoulli beam can be shown by the following equation:

$$E_S I\frac{\partial^4 w}{\partial x^4}+\frac{\partial^2 M_p}{\partial x^2}+(\rho_F+\rho_S)A\frac{\partial^2 w}{\partial t^2}=f(x,t) \qquad (20)$$

$$I\frac{\partial^3 w}{\partial x^2\partial t}+\frac{n_F^2}{S_V}\frac{\partial^2 M_p}{\partial x^2}=0 \qquad (21)$$

where E_S, ρ_F, ρ_S, n_F and S_V are respectively Young's modulus of the solid constituent, partial densities of the fluid and solid constituents, respectively, volume fraction of the fluid phase, and the interaction coefficient between the solid skeleton and the pore fluid.

$$S_V=\gamma n_F^2/K_F \qquad (22)$$

where γ is the dynamic viscosity of the fluid and K_F is permeability under dynamic and quasi-static conditions. $F(x, t)$ is defined in Equation (2) and the equivalent couple of the fluid pore pressure p, i.e., M_p, is defined as follows:

$$M_p=\iint_A zp\,dy\,dz \qquad (23)$$

For the poroelastic beam with an attached mass-spring system, Equations (20), (21), and (4) should be solved in conjunction with Equation (2).

Both the ends of the beam are supposed to be permeable and one end is non-ideal simply supported. Therefore, the fluid pressure boundary conditions are consequently,

$$M_p(0,t)=M_p(L,t)=0 \qquad (24)$$

$$w(0,t)=0,\quad \frac{\partial^2 w(0,t)}{\partial x^2}=0 \qquad (25)$$

$$w(L,t)=\varepsilon_1\sin(bt),\quad \frac{\partial^2 w(L,t)}{\partial x^2}=\varepsilon_2\sin(bt) \qquad (26)$$

Initial values of all parameters are supposed to be zero, except for

$$y(0)=y_0 \qquad (27)$$

3. Analytical solutions of the three types of governing equations

3.1. The elastic Euler-Bernoulli beam

Transverse deflection of the beam $w(x,t)$ may be resolved into two parts as follows:

$$w(x,t)=u(x,t)+v(x,t) \qquad (28)$$

where the function $v(x, t)$ may be defined as follows:

$$v(x,t)=\left[\left(\frac{\varepsilon_2 L^2}{6}-\varepsilon_1\right)\left(\frac{x}{L}\right)^4+\left(2\varepsilon_1-\frac{\varepsilon_2 L^2}{6}\right)\left(\frac{x}{L}\right)^3\right]\sin(bt) \tag{29}$$

Indeed, solving $w(x, t)$ like Equation (28) makes the process of application of the finite Fourier sine transform slightly easier because the definition of $v(x, t)$ in the form of Equation (29) gives a partial differential equation in terms of $u(x, t)$ with homogeneous boundary conditions.

Substitution of Equations (28) and (29) into Equations (3) and (4) gives the following equations:

$$EI\frac{\partial^4 u}{\partial x^4}+\rho A\frac{\partial^2 u}{\partial t^2}-P\frac{\partial^2 u}{\partial x^2}=m(g-\ddot{y})\delta(x-x_o)+f_0\delta(x-Vt)-h(x,t) \tag{30a}$$

$$u(x,0)=g_1(x),\qquad \frac{\partial u(x,0)}{\partial t}=g_2(x)-b\left[\left(\frac{\varepsilon_2 L^2}{6}-\varepsilon_1\right)\left(\frac{x}{L}\right)^4+\left(2\varepsilon_1-\frac{\varepsilon_2 L^2}{6}\right)\left(\frac{x}{L}\right)^3\right] \tag{30b}$$

$$u(0,t)=0,\qquad \frac{\partial^2 u(0,t)}{\partial^2 x}=0,\qquad u(L,t)=0,\qquad \frac{\partial^2 u(L,t)}{\partial x^2}=0 \tag{30c}$$

where,

$$h(x)=EI\frac{\partial^4 v}{\partial x^4}+\rho A\frac{\partial^2 v}{\partial t^2}-P\frac{\partial^2 v}{\partial x^2} \tag{31}$$

Applying Laplace transform to Equations (4), (30a), and (30c) gives the following:

$$EI\frac{\partial^4 U}{\partial x^4}-P\frac{\partial^2 U}{\partial x^2}+\rho A\left[s^2U-su(x,0)-\frac{\partial u}{\partial t}(x,0)\right]=m\left(\frac{g}{s}-s^2Y+sy_0\right)\delta(x-x_0)-H(x,s) \tag{32}$$

$$ms^2Y-msy_0+kY=kW(x_0,s) \tag{33}$$

$$U(0,s)=0,\qquad \frac{\partial^2 U(0,s)}{\partial^2 x}=0,\qquad U(L,s)=0,\qquad \frac{\partial^2 U(L,s)}{\partial x^2}=0 \tag{34}$$

where, U and Y stand for the transformed version of the corresponding functions. Finding Y from Equation (33) and substituting it into Equation (32) gives the following:

$$EI\frac{\partial^4 U}{\partial x^4}-P\frac{\partial^2 U}{\partial x^2}+\rho As^2U=m\left[\frac{g}{s}-s^2\left(\frac{kW(x_0,s)+msy_0}{ms^2+k}\right)+sy_0\right]\delta(x-x_0)+G(x,s) \tag{35}$$

where,

$$G(x,s)=-H(x,s)+\rho A\left[su(x,0)+\frac{\partial u}{\partial t}(x,0)\right] \tag{36}$$

In order to obtain a compact equation, Equation (35) can be rewritten as follows:

$$EI\frac{\partial^4 U}{\partial x^4}-P\frac{\partial^2 U}{\partial x^2}+\rho As^2U=\mathcal{F}(x_0,s)\delta(x-x_0)+G(x,s) \tag{37}$$

where,

$$\mathcal{F}(x_0,s)=\mathcal{A}-\mathcal{B}W(x_0,s) \tag{38}$$

where in,

$$\mathcal{A} = m\frac{(mg+ky_0)s^2+kg}{s(ms^2+k)} \quad (39)$$

$$\mathcal{B} = \frac{mks^2}{ms^2+k} \quad (40)$$

To complete the solution process of the problem, the finite Fourier sine transform with the following definition was used [36]:

$$F_s[f(x);n] = \bar{f}_s(n) = \int_0^a f(x)\sin\left(\frac{n\pi x}{a}\right)dx \quad (41)$$

whose inverse transform may be obtained from the following equation:

$$F_s^{-1}\left[\bar{f}_s(n);x\right] = f(x) = \frac{2}{a}\sum_{n=1}^{\infty}\bar{f}_s(n)\sin\left(\frac{n\pi x}{a}\right) \quad (42)$$

Employing the integration by parts rule, the following relation is derived when *f*(*a*)= *f*(0)= 0, as per the definition presented in Equation (41):

$$F_s\left[\frac{d^4 f}{dx^4};n\right] = \frac{n^4\pi^4}{a^4}\bar{f}_s(n) \quad (43)$$

Thus, imposing the boundary conditions presented in Equation (34) based on Equations (41) and (43) at *a*=*L*, the transformed form of Equation (37) may be written as follows:

$$\left(EI\frac{n^4\pi^4}{L^4}+P\frac{n^2\pi^2}{L^2}+\rho As^2\right)\bar{U}_s(n,s) = \mathcal{F}(x_0,s)\sin\left(\frac{n\pi x_0}{L}\right)+\bar{G}_s(n,s) \quad (44)$$

Obtaining $\bar{U}_s(n,s)$ from Equation (44) and applying the inverse Fourier transform defined in Equation (42) gives the following solution:

$$F_s^{-1}\left[\bar{U}_s(n,s);x\right] = U(x,s) = \frac{2}{L}\sum_{n=1}^{\infty}\frac{\mathcal{F}(x_0,s)\sin\left(\frac{n\pi x_0}{L}\right)+\bar{G}_s(n,s)}{EI\frac{n^4\pi^4}{L^4}+P\frac{n^2\pi^2}{L^2}+\rho As^2}\sin\left(\frac{n\pi x}{L}\right) \quad (45)$$

According to Equation (28), Equation (38) can be rewritten as follows:

$$\mathcal{F}(x_0,s) = \mathcal{A}-\mathcal{B}V(x_0,s)-\mathcal{B}U(x_0,s) \quad (46)$$

where,

$$V(x_0,s) = L[v(x_0,t)] = \frac{b}{s^2+b^2}\left[\left(\frac{\varepsilon_2 L^2}{6}-\varepsilon_1\right)\left(\frac{x_0}{L}\right)^4+\left(2\varepsilon_1-\frac{\varepsilon_2 L^2}{6}\right)\left(\frac{x_0}{L}\right)^3\right] \quad (47)$$

Rewriting Equation (45) based on Equation (46) gives the following:

$$U(x,s) = \frac{2}{L}\sum_{n=1}^{\infty}\frac{\left[\mathcal{A}-\mathcal{B}U(x_0,s)-\mathcal{B}V(x_0,s)\right]\sin\left(\frac{n\pi x_0}{L}\right)+\bar{G}_s(n,s)}{EI\frac{n^4\pi^4}{L^4}+P\frac{n^2\pi^2}{L^2}+\rho As^2}\sin\left(\frac{n\pi x}{L}\right) \quad (48)$$

Notably, in Equation (48), *U*(*x*, *s*) appeared at the left hand side of the equation while a relevant $U(x_0,s)$ term merged at the right hand side of the mentioned equation. To find a $U(x,s)$ expression independent of $U(x_0,s)$, Equation (48) may be used as it is a general form for $U(x,s)$, which is true for all $x \in [0,L]$ including x_0. Thus, to find an independent expression for $U(x,s)$, x must be replaced by x_0 at both the sides of Equation (48) to find an expression for $U(x_0,s)$ and then substituting it into the right hand side of Equation (48). Conducting some manipulations, the following results were obtained:

$$U(x_0,s)=\frac{F_1(x_0,s)+F_3(x_0,s)}{1+F_2(x_0,s)} \tag{49}$$

where,

$$F_1(x_0,s)=\frac{2}{L}\sum_{n=1}^{\infty}\frac{\mathcal{A}-\mathcal{B}V(x_0,s)}{EI\dfrac{n^4\pi^4}{L^4}+P\dfrac{n^2\pi^2}{L^2}+\rho As^2}\sin^2\left(\frac{n\pi x_0}{L}\right) \tag{50}$$

$$F_2(x_0,s)=\frac{2}{L}\sum_{n=1}^{\infty}\frac{\mathcal{B}}{EI\dfrac{n^4\pi^4}{L^4}+P\dfrac{n^2\pi^2}{L^2}+\rho As^2}\sin^2\left(\frac{n\pi x_0}{L}\right) \tag{51}$$

$$F_3(x_0,s)=\frac{2}{L}\sum_{n=1}^{\infty}\frac{\overline{G}_s(n,s)}{EI\dfrac{n^4\pi^4}{L^4}+P\dfrac{n^2\pi^2}{L^2}+\rho As^2}\sin\left(\frac{n\pi x_0}{L}\right) \tag{52}$$

Substituting $U(x_0,s)$ from Equation (49) into Equation (48) gives the final form of $U(x,s)$. After applying the inverse Laplace transform, $u(x,t)$ can be obtained and, consequently, $w(x,t)$ can be found from Equation (29).

3.2. The elastic Timoshenko beam

The process of establishing the analytical solution of the elastic Timoshenko beam is almost similar to that of the elastic Euler-Bernoulli beam. After resolving $w(x,t)$ into two parts like in Equation (28), $v(x,t)$ may be defined as follows:

$$v(x,t)=\left[\left(\frac{\varepsilon_3 L^2}{6}-\varepsilon_1\right)\left(\frac{x}{L}\right)^4+\left(2\varepsilon_1-\frac{\varepsilon_3 L^2}{6}\right)\left(\frac{x}{L}\right)^3\right]\sin(bt)\ ,\qquad \varepsilon_3=\varepsilon_2-\frac{\rho b^2}{\kappa G}\varepsilon_1 \tag{53}$$

Substituting Equation (53) into Equation (8), imposing the boundary conditions (16,17) and the initial conditions (18, 19) and the Laplace transform on the resulting equation, as well as by substituting Y from the Laplace transformed version of Equation (4) into the transformed version of the governing equation of Timoshenko beam gives the following equation:

$$\begin{aligned}
&EI\frac{\partial^4U}{\partial x^4}-\left[P+\rho I\left(1+\frac{E}{\kappa G}\right)\right]s^2\frac{\partial^2U}{\partial x^2}+\left(\rho As^2+\frac{\rho^2 I}{\kappa G}s^4\right)U=\\
&\quad-\frac{EI}{\kappa AG}m\left[\frac{g}{s}-s^2\left(\frac{kW(x_0,s)+msy_0}{ms^2+k}\right)+sy_0\right]\delta^{(2)}(x-x_0)\\
&\quad-\frac{\rho I}{\kappa AG}m\left[s^4\left(\frac{kW(x_0,s)+msy_0}{ms^2+k}\right)-s^3y_0\right]\delta(x-x_0)\\
&\quad+m\left[\frac{g}{s}-s^2\left(\frac{kW(x_0,s)+msy_0}{ms^2+k}\right)+sy_0\right]\delta(x-x_0)+G_1(x,s)
\end{aligned} \tag{54}$$

where,

$$G_1(x,s)=\left(-\frac{EI}{\kappa AGV^2}-\frac{\rho I}{\kappa AG}+\frac{1}{s^2}\right)\frac{f_0 s^2}{V}e^{-\frac{sx}{V}}$$
$$+\rho A\left\{s\,g_1(x)+g_2(x)-b\left[\left(\frac{\varepsilon_3 L^2}{6}-\varepsilon_1\right)\left(\frac{x}{L}\right)^4+\left(2\varepsilon_1-\frac{\varepsilon_3 L^2}{6}\right)\left(\frac{x}{L}\right)^3\right]\right\}$$
$$-\rho I\left(1+\frac{E}{\kappa G}\right)\left(s\frac{\partial^2 g_1(x)}{\partial x^2}+\frac{\partial^2}{\partial x^2}\left\{g_2(x)-b\left[\left(\frac{\varepsilon_3 L^2}{6}-\varepsilon_1\right)\left(\frac{x}{L}\right)^4+\left(2\varepsilon_1-\frac{\varepsilon_3 L^2}{6}\right)\right.\right.\right. \tag{55}$$
$$\left.\left.\left.\left(\frac{x}{L}\right)^3\right]\right\}\right)+\frac{\rho^2 I}{\kappa G}\left(s^3 g_1(x)+s^2\left\{g_2(x)-b\left[\left(\frac{\varepsilon_3 L^2}{6}-\varepsilon_1\right)\left(\frac{x}{L}\right)^4+\left(2\varepsilon_1-\frac{\varepsilon_3 L^2}{6}\right)\right.\right.\right.$$
$$\left.\left.\left.\left(\frac{x}{L}\right)^3\right]\right\}\right)+b^3\left[\left(\frac{\varepsilon_3 L^2}{6}-\varepsilon_1\right)\left(\frac{x}{L}\right)^4+\left(2\varepsilon_1-\frac{\varepsilon_3 L^2}{6}\right)\left(\frac{x}{L}\right)^3\right]\Bigg)-H_1(x,s)$$

where,

$$H_1(x,t)=L\left(EI\frac{\partial^4 v}{\partial x^4}-P\frac{\partial^2 v}{\partial x^2}+\rho A\frac{\partial^2 v}{\partial t^2}-\rho I\left(1+\frac{E}{\kappa G}\right)\frac{\partial^4 v}{\partial x^2\partial t^2}+\frac{\rho^2 I}{\kappa G}\frac{\partial^4 v}{\partial t^4}\right) \tag{56}$$

Applying the finite Fourier sine transform to Equation (54) gives the following equation:

$$\psi(n,s)\overline{U}_s(n,s)=\left[A_1(n,s)-B_1(n,s)W(x_0,s)\right]\sin\left(\frac{n\pi x_0}{L}\right)+\overline{G}_1(n,s) \tag{57}$$

where,

$$\psi(n,s)=EI\frac{n^4\pi^4}{L^4}+\left[P+\rho I\left(1+\frac{E}{\kappa G}\right)\right]s^2\frac{n^2\pi^2}{L^2}+\left(\rho A s^2+\frac{\rho^2 I}{\kappa G}s^4\right) \tag{58}$$

$$A_1(n,s)=m\left(\frac{g}{s}+\frac{ksy_0}{ms^2+k}\right)+\frac{EIm}{\kappa AG}\left(\frac{g}{s}+\frac{ksy_0}{ms^2+k}\right)\frac{n^2\pi^2}{L^2}+\frac{\rho I}{\kappa AG}\frac{kms^3 y_0}{ms^2+k} \tag{59}$$

$$B_1(n,s)=\frac{mks^2}{ms^2+k}\left(1+\frac{EIm}{\kappa AG}\frac{n^2\pi^2}{L^2}+\frac{\rho I}{\kappa AG}\right) \tag{60}$$

Therefore,

$$U(x,s)=\frac{2}{L}\sum_{n=1}^{\infty}\frac{[A_1-B_1U(x_0,s)-B_1V(x_0,s)]\sin\left(\frac{n\pi x_0}{L}\right)+\overline{G}_s(n,s)}{\psi(n,s)}\sin\left(\frac{n\pi x}{L}\right) \tag{61}$$

Such that

$$U(x_0,s)=\frac{F_4(x_0,s)+F_6(x_0,s)}{1+F_5(x_0,s)} \tag{62}$$

where,

$$F_4(x_0,s)=\frac{2}{L}\sum_{n=1}^{\infty}\frac{A_1(n,s)-B_1(n,s)V(x_0,s)}{\psi(n,s)}\sin^2\left(\frac{n\pi x_0}{L}\right) \tag{63}$$

$$F_5(x_0,s)=\frac{2}{L}\sum_{n=1}^{\infty}\frac{B_1(n,s)}{\psi(n,s)}\sin^2\left(\frac{n\pi x_0}{L}\right) \tag{64}$$

$$F_6(x_0,s)=\frac{2}{L}\sum_{n=1}^{\infty}\frac{\overline{G}_s(n,s)}{\psi(n,s)}\sin\left(\frac{n\pi x_0}{L}\right) \tag{65}$$

As in the previous case, substituting $U(x_0,s)$ from Equation (62) into Equation (61), the final form of $U(x,s)$ can be obtained. After imposing the inverse Laplace transform on this expression, $u(x,t)$ can be derived and consequently $w(x,t)$ can be determined based on Equation (28).

3.3. The poroelastic beam

Combining Equations (20) and (21) gives the following equation that is in terms of the lateral deflection of the beam (i.e., w) only.

$$E_S I\frac{\partial^4 w}{\partial x^4}-\frac{IS_V}{n_F^2}\frac{\partial^3 w}{\partial x^2\partial t}+(\rho_F+\rho_S)\,A\frac{\partial^2 w}{\partial t^2}=m\left[g-\ddot{y}(t)\right]\delta\left(x-x_o\right)+f_0\,\delta(x-Vt) \tag{66}$$

Therefore, the associated governing equations and the initial and boundary conditions may be summarized as follows:

$$E_S I\frac{\partial^4 w}{\partial x^4}-\frac{IS_V}{n_F^2}\frac{\partial^3 w}{\partial x^2\partial t}+(\rho_F+\rho_S)\,A\frac{\partial^2 w}{\partial t^2}=m\left[g-\ddot{y}(t)\right]\delta\left(x-x_o\right)+f_0\,\delta(x-Vt) \tag{67}$$

$$m\ddot{y}+k\,y=k\,w(x_0,t) \tag{68}$$

$$y(0)=y_0\,,\qquad \dot{y}(0)=0\,,\qquad w\left(x,0\right)=0\,,\qquad \dot{w}\left(x,0\right)=0 \tag{69}$$

$$w\,(0,t)=0,\qquad \frac{\partial^2 w\,\left(0,t\right)}{\partial x^2}=0\,,\quad w\,(L,t)=\varepsilon_1\sin(bt),\qquad \frac{\partial^2 w\,\left(L,t\right)}{\partial x^2}=\varepsilon_2\,\sin(bt) \tag{70}$$

Finding an analytical solution for the system of Equations (67)-(70) is achievable by following the mathematical procedure presented in the previous sections. In this regard, after resolving $w(x,\ t)$ into two parts like in Equations (28) and (29), Equations (67), (69), and (70) may be rewritten based on the new variables u(x,t) and v(x,t) as follows:

$$E_S I\frac{\partial^4 u}{\partial x^4}-\frac{IS_V}{n_F^2}\frac{\partial^3 u}{\partial x^2\partial t}+(\rho_F+\rho_S)\,A\frac{\partial^2 u}{\partial t^2}=m\left(g-\ddot{y}\right)\delta\left(x-x_o\right)+f_0\delta(x-Vt)-h(x,t) \tag{71}$$

$$u\left(x,0\right)=g_1(x)\,,\qquad \frac{\partial u\left(x,0\right)}{\partial t}=g_2(x)-b\left[\left(\frac{\varepsilon_2 L^2}{6}-\varepsilon_1\right)\left(\frac{x}{L}\right)^4+\left(2\varepsilon_1-\frac{\varepsilon_2 L^2}{6}\right)\left(\frac{x}{L}\right)^3\right] \tag{72}$$

$$u\left(0,t\right)=0,\qquad \frac{\partial^2 u\left(0,t\right)}{\partial^2 x}=0\,,\qquad u\left(L,t\right)=0\,,\qquad \frac{\partial^2 u\left(L,t\right)}{\partial x^2}=0 \tag{73}$$

where,

$$h(x,t)=E_S I\frac{\partial^4 v}{\partial x^4}-\frac{IS_V}{n_F^2}\frac{\partial^3 v}{\partial x^2\partial t}+(\rho_F+\rho_S)\,A\frac{\partial^2 v}{\partial t^2} \tag{74}$$

Applying Laplace transform to Equation (71)gives the following equation:

$$E_S I \frac{\partial^4 U}{\partial x^4} - \frac{IS_V s}{n_F^2}\frac{\partial^2 U}{\partial x^2} + (\rho_F + \rho_S)As^2 U = \mathcal{F}(x_0, s)\delta\left(x - x_0\right) + G(x, s) \tag{75}$$

where,

$$G(x,s) = -H(x,s) + (\rho_F + \rho_S)A\left[su(x,0) + \frac{\partial u}{\partial t}(x,0)\right] \tag{76}$$

In Equation (75), $\mathcal{F}(x_0, s)$ may be defined according to Eq. (38). In order to complete the solution procedure of the problem, the finite Fourier sine transform can be used, such that

$$U(x,s) = \frac{2}{L}\sum_{n=1}^{\infty}\frac{[\mathcal{A} - \mathcal{B}U(x_0,s) - \mathcal{B}V(x_0,s)]\sin\left(\frac{n\pi x_0}{L}\right) + \overline{G}_s(n,s)}{E_S I \frac{n^4\pi^4}{L^4} + \frac{IS_V s}{n_F^2}\frac{n^2\pi^2}{L^2} + (\rho_F + \rho_S)As^2}\sin\left(\frac{n\pi x}{L}\right) \tag{77}$$

So that,

$$U(x_0,s) = \frac{2}{L}\sum_{n=1}^{\infty}\frac{[\mathcal{A} - \mathcal{B}U(x_0,s) - \mathcal{B}V(x_0,s)]\sin\left(\frac{n\pi x_0}{L}\right) + \overline{G}_s(n,s)}{E_S I \frac{n^4\pi^4}{L^4} + \frac{IS_V s}{n_F^2}\frac{n^2\pi^2}{L^2} + (\rho_F + \rho_S)As^2}\sin\left(\frac{n\pi x_0}{L}\right) \tag{78}$$

With few manipulations, the following equation is achieved:

$$U(x_0,s) = \frac{F_1(x_0,s) + F_3(x_0,s)}{1 + F_2(x_0,s)} \tag{79}$$

where,

$$F_1(x_0,s) = \frac{2}{L}\sum_{n=1}^{\infty}\frac{\mathcal{A} - \mathcal{B}V(x_0,s)}{E_S I \frac{n^4\pi^4}{L^4} + \frac{IS_V s}{n_F^2}\frac{n^2\pi^2}{L^2} + (\rho_F + \rho_S)As^2}\sin^2\left(\frac{n\pi x_0}{L}\right) \tag{80}$$

$$F_2(x_0,s) = \frac{2}{L}\sum_{n=1}^{\infty}\frac{\mathcal{B}}{E_S I \frac{n^4\pi^4}{L^4} + \frac{IS_V s}{n_F^2}\frac{n^2\pi^2}{L^2} + (\rho_F + \rho_S)As^2}\sin^2\left(\frac{n\pi x_0}{L}\right) \tag{81}$$

$$F_3(x_0,s) = \frac{2}{L}\sum_{n=1}^{\infty}\frac{\overline{G}_s(n,s)}{E_S I \frac{n^4\pi^4}{L^4} + \frac{IS_V s}{n_F^2}\frac{n^2\pi^2}{L^2} + (\rho_F + \rho_S)As^2}\sin\left(\frac{n\pi x_0}{L}\right) \tag{82}$$

Substituting $U(x_0,s)$ from Eq. (78) into Equation (77) gives the final form of $U(x,s)$, such that application of the inverse Laplace transform gives $u(x,t)$ and, consequently, $w(x,t)$ based on Equation (28).

4. Results and Discussions

4.1. Verification of the results

The considered general problem consists of several aspects that have not been combined fully or even partially in any prior research. This point makes verification of the results of the presented formulation a formidable task. The poroelasticity, non-ideal support, attached mass, and moving load are among some of these parameters. For this reason, dynamic deflection results of a simply supported beam without attached mass-spring system (i.e., $\varepsilon_1 = \varepsilon_2 = 0$ and $m = 0$) having ideal supports were compared with the results of Fryba [37] under the action of a moving load.

Fryba [37] presented a closed-form solution for simple elastic Euler-Bernoulli beams under moving loads:

$$w(x,t) = \frac{f_0 L^3}{48EI} \sum_{j=1}^{\infty} \frac{1}{j^2 (j^2 - \alpha^2)} \left(\sin j\omega t - \frac{\alpha}{j} \sin \omega_j t \right) \sin\left(\frac{j\pi x}{L} \right) \tag{83}$$

where,

$$\alpha = \frac{VL}{\pi}\sqrt{\frac{\rho A}{EI}}, \qquad \omega = \frac{\pi V}{L}, \qquad \omega_j = \frac{j^2 \pi^2}{L^2}\sqrt{\frac{EI}{\rho A}} \tag{84}$$

Figure 2 presents the comparison of the present results with those of a previous paper [37] as follows:

$L = 1m$, $a = 50mm$, $h = 10mm$, $k_1 = 5/6$, $\rho = 7800kg/m^{-3}$, $G = 48GPa$, $E = 210GPa$, $\varepsilon_1 = \varepsilon_2 = 0$, $m = 0$, $f_0 = 10N$, $V = 1m/s$

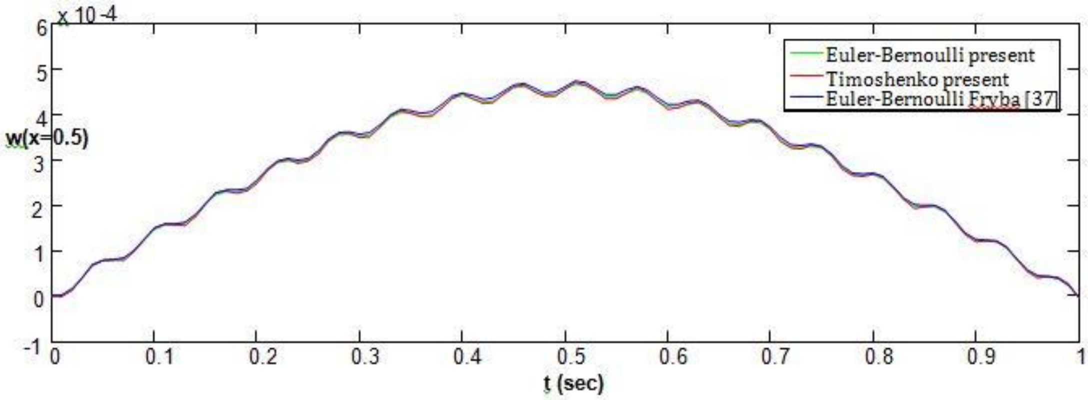

Fig. 2. Comparison between the lateral deflection results of the present study and those of a previous study [37] for an elastic beam without attached mass-spring system and non-ideal supports under the action of a moving load

In this regard, the present results for the elastic Euler-Bernoulli and elastic Timoshenko beams have been compared with the results of a previous study [37]. Fryba [37] derived the response of the Euler-Bernoulli beam based on the Fourier finite sine integral transformation in the time domain. As shown in Figure 2, the present results are almost coincident with the results of Fryba for the Euler-Bernoulli beam. Deviations of results of Timoshenko beam from the results of Fryba were <1%. Therefore, all three types of results are in excellent agreement.

4.2. Results of the elastic Timoshenko and Euler-Bernoulli beams

The present section discusses the observations of the investigation of some parameters that have not been considered previously, including the non-ideal supports and the attached mass-spring system. A comprehensive parametric study was accomplished to extract practical conclusions. Consider the case of an elastic beam with attached mass and a moving load, with the following geometric, material, and stiffness specifications:

$L = 1m$, $a = 50mm$, $h = 10mm$, $\rho = 7800kg/m^3$, $G = 48GPa$, $E = 210GPa$, $m = 5kg$, $\varepsilon_1 = \varepsilon_2 = 0$, $k = 5000N/m$, $k_1 = 5/6$, $f_0 = 50N$, $x_0 = 0.5m$, $y_0 = 0$.

where a and h are respectively, width and height (thickness) of the beam section. Therefore, the mass of the beam was 3.9 kg. Since the beam is thin, as Figure 2 implies, almost no noticeable differences were observed between the responses of Timoshenko and Euler-Bernoulli two theories; therefore, only the results of the Timoshenko beam will be illustrated in some of the figures cited subsequently.

4.2.1. Influence of the magnitude of the attached mass

The effects of the magnitude of the attached mass on time history of the lateral deflection of the mid-point of the beam are illustrated in Fig. 3 for an elastic beam with the information mentioned in the foregoing section and $f_0 = 50N, V = 1m/s$.

As shown in Figure 3, the influence of the magnitude of the mass of the attached mass-spring system on the fundamental natural frequency of the multi-body system is negligible; but, this parameter significantly affects the amplitude of the vibration of the beam under a moving load such that the amplitude increases in proportion with the amount of the attached mass. This phenomenon is partially monitored by the in-phase and anti-phase relative vibration modes of the beam and the attached mass.

4.2.2. Effects of parameters of the non-ideal support

In the present section, the effects of the existence of non-ideal (with transverse and moment-type excitations) supports and the relevant values of the parameters were investigated. To avoid any influences on the results of interaction between the moving load and the non-ideal support excitations, a beam without any moving load was used to observe the effects of the non-ideal support more clearly. The effects of the non-ideal supports on the responses of a beam with a moving load have been discussed in the next section, where the more general case of a poroelastic beam with a moving load and an attached mass-spring system has been considered. Specifications of the resulting multi-body system are similar to those mentioned in the previous sections, expect for the following information:

$$y_0 = 0.005m, \quad \varepsilon_1 = \varepsilon_2 = 0.005, \quad b = 10.$$

Time variations of the lateral deflection of the middle point of a Timoshenko beam with an non-ideal support (Fig. 1), whose general specification are mentioned in the previous sections, are demonstrated in Figure 4 for different ε values ($y_0 = 0.005$). As expected, the amplitude of the vibration was proportional with the amplitude of the applied excitations; however, the amplitude of the superimposed vibrations that performed with the fundamental natural frequency experienced only small changes. Therefore, the total amplitude of the vibration did not vary proportional to the amplitude of the excitations as implied by Figure 4.

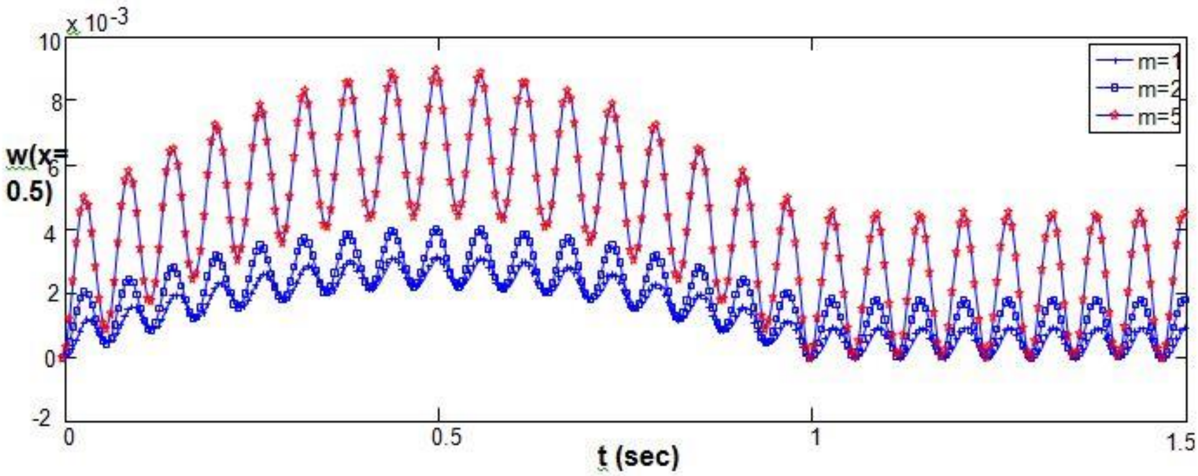

Fig. 3. Vibration of a Timoshenko beam with an attached mass-spring system and an ideal support under a moving load ($f_0 = 50N, V = 1m/s$ and $m = 1, 2, 5kg$)

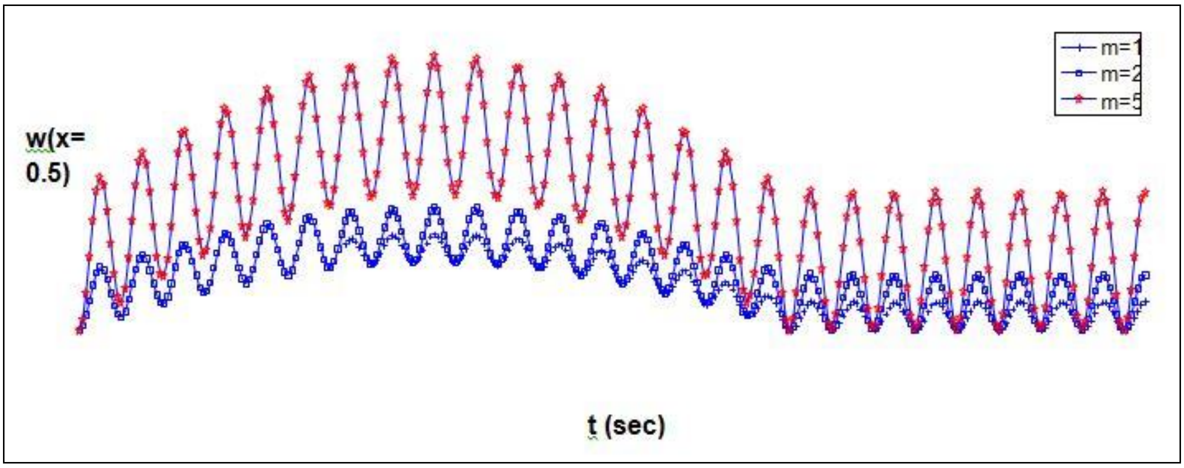

Fig. 4. Time variations of the lateral deflection of the middle point of a Timoshenko beam with an attached mass-spring system and a non-ideal support ($\varepsilon_1 = \varepsilon_2 = Eps, b = 10, x_0 = 0.5$ **)**

4.3. Results of the Poroelastic beam

In the present section, the more general case of a poroelastic beam with an attached mass-spring system was considered. Various cases (e.g., free and forced vibration of beams with or without non-ideal conditions) were considered to enable a parametric study, with $\gamma = 10^{-3}$ Ns/m^2 for water.

4.3.1. Free vibration

Free vibration is usually considered to identify characteristics of the transient response of a structure. We considered the solid and fluid phases of the beam structure as wood and water, respectively. Due to the existence of a wide range of wood types, the approximate material properties of the resulting porous structure as well as the kinematic and dynamic parameters were selected as follows:

$$n_f = 0.23,\ g = 10m/s^2;\ a = h = 20mm,\ E = 13GPa,\ \rho_s + \rho_f = 1000kg/m^3,\ y_0 = 5mm,$$
$$K_F = 10^{-9}, x_0 = 0.5m,\ \varepsilon_1 = \varepsilon_2 = 0,\ m = 0.02kg,\ k = 500N/m.$$

To present the effects of poroelasticity of the material properties, beam supports were temporary assumed to be ideal. The transient lateral deflection response of the poroelastic beam due to imposing of an initial displacement to the attached mass has been illustrated in Figure 5. As shown in Figure 5, the resulting free vibrations disappear with time. The beat-type oscillations observed can be attributed to the presence of the suspended mass.

To demonstrate the damping effect of the poroelastic material, the response of the beam has been plotted for $n_F = 0$ in Figure 6. This response corresponds to that of an elastic Euler-Bernoulli beam. Notably, as in Figure 6, in contrast to the response shown in Figure 5, oscillations of the beam accomplished without any suppression in the vibration amplitude. Effect of the magnitude of the suspended mass on free vibration of the poroelastic beam has been shown in Figure 7. Figure 7 also reveals that, due to altering of the differences between the fundamental and subsequent natural frequencies by changing the magnitude of the suspended mass, the beat-type oscillation may become an overall vibration with a superimposed minor oscillation associated with the higher vibration modes or a quite disorder vibration whose effects of the higher modes are more pronounced (a vibration with significant local oscillations).

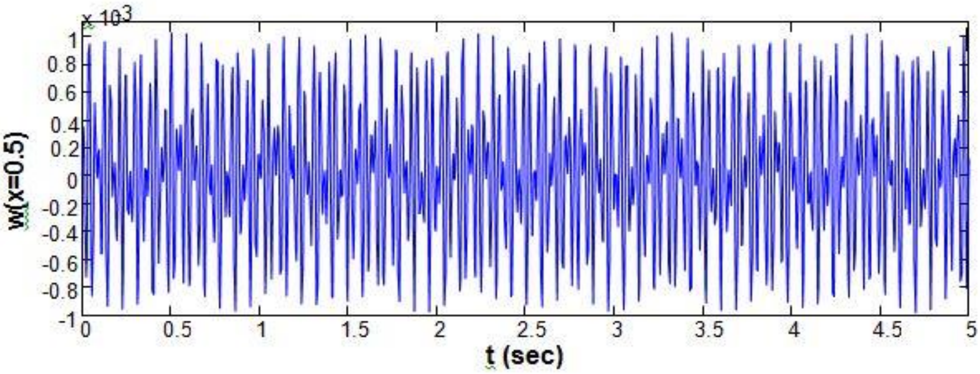

Fig. 5. Free vibration of a poroelastic beam with an attached mass-spring system and an ideal support ($y_0 = 0.005m$)

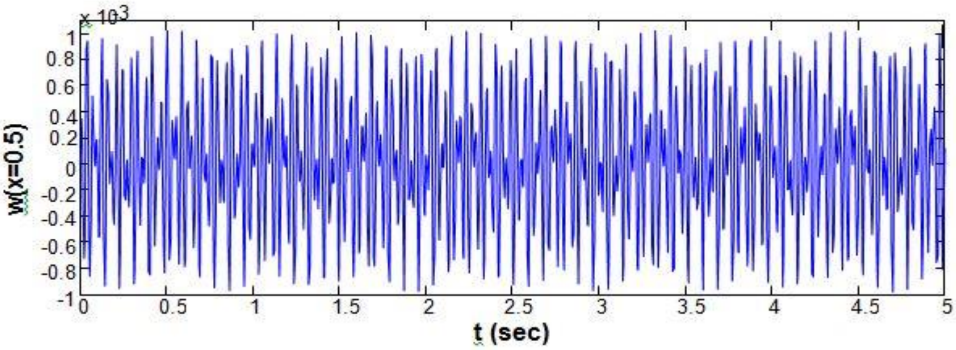

Fig. 6. Free vibration of an elasticEuler-Bernoulli beam with an attached mass-spring system and an ideal support ($y_0 = 0.005m$)

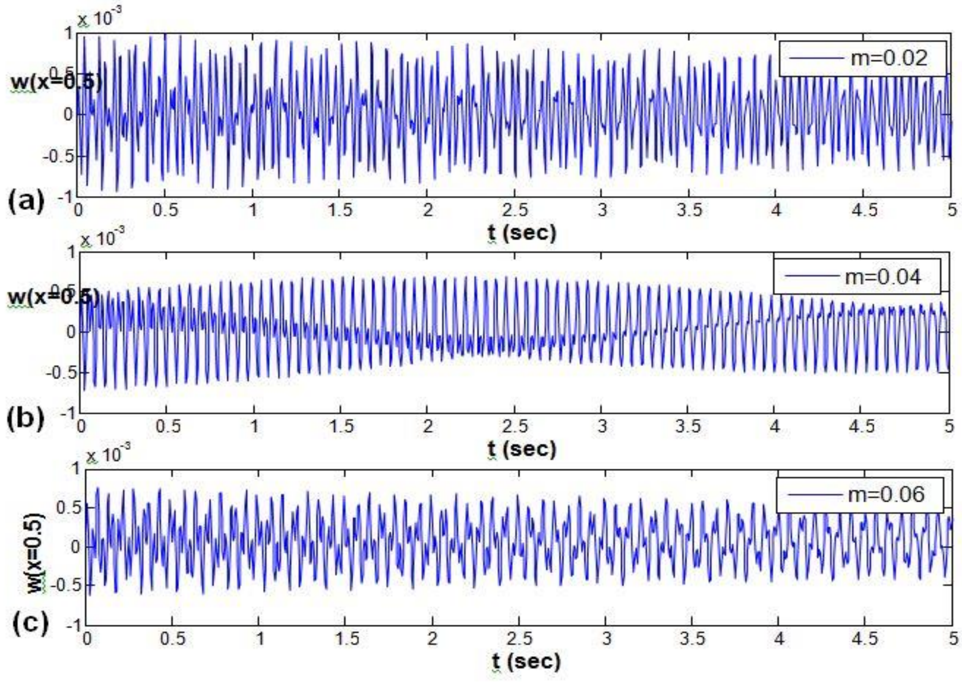

Fig. 7. Effects of the magnitude of a suspended mass on the free vibration of a poroelastic beam with an ideal support ($y_0 = 0.005m$):a) beat-type oscillations, b) a global vibration with local superimposed oscillations, and c) a vibration with pronounced local oscillations

4.3.2. Effect of a moving load (forced vibration)

In this section, forced vibration of a poroelastic beam with zero initial and boundary conditions under a moving load was investigated. The employed geometric, material, and vibration information was as follows:

$$n_F = 0.23,\ g = 10m/s^2,\ a = h = 20mm,\ E = 13GPa,\ \rho_s + \rho_f = 1000kg/m^3,\ y_0 = 0,$$
$$K_F = 5\times10^{-10},\ x_0 = 0.5m,\ \varepsilon_1 = \varepsilon_2 = 0,\ m = 0.02kg,\ k = 500N/m.$$

In this regard, the effects of both magnitude and speed of a moving load on the lateral deflection response was studied (results are given in Fig. 8). As shown in Fig. 8, it may be deduced that, generally, the amplitude of the resulting vibration is not proportional to the magnitude of the moving load and that the moving speed only slightly affects the vibration amplitude. Furthermore, damping of the transient vibration following passage of the load is noticeable. Moreover, when the load passes at a higher velocity, the amplitude of the vibration at the moment of leaving the beam becomes greater, because damping of the energy induced by a moving load to the beam, due to poroelasticity nature of the materials, is more remarkable when this energy is subjected to damping for a longer passage time.

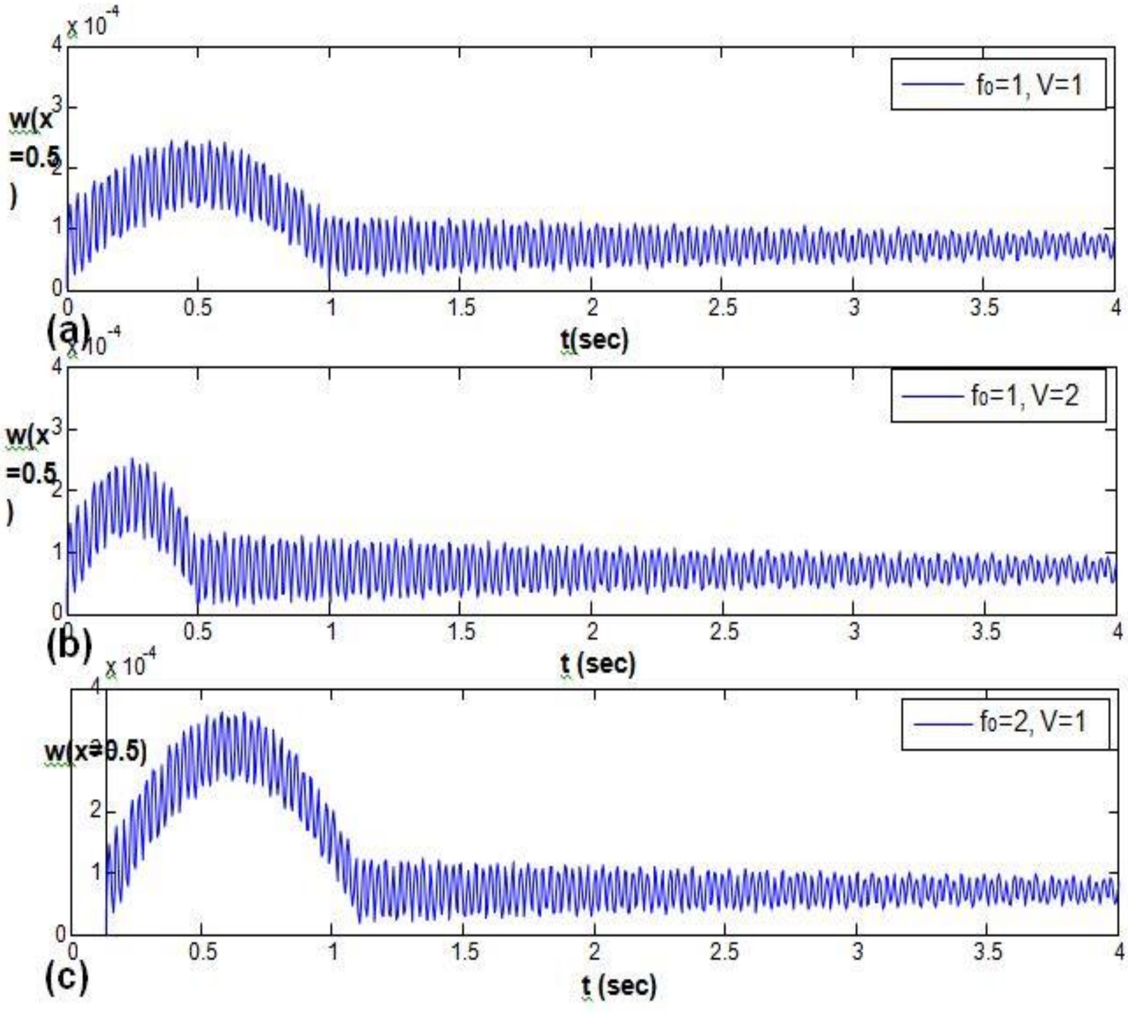

Fig. 8. Influence of both the magnitude and speed of a moving load on the vibration of a poroelastic beam with an attached mass-spring system and ideal supports

4.3.3. Effect of the non-ideal support on vibration of poroelastic beam

Finally, the most general case of a poroelastic beam with an attached mass-spring system and a non-ideal support subjected to a moving concentrated force was considered. The beam was initially at a stationary situation. Time variations of the lateral deflection of the middle point of the poroelastic beam have been plotted in Fig. 9 for the following material, geometric, and dynamic parameters:

$$n_F = 0.23,\ g = 10m/s^2,\ a = h = 20mm\ ;\ E = 13GPa, \rho_s + \rho_f = 1000kg/m^3,\ y_0 = 0,$$
$$K_f = 5\times10^{-10}, x_0 = 0.5m, b = 10, m = 0.02kg, k = 500N/m, f_0 = 10, V = 1m/s$$

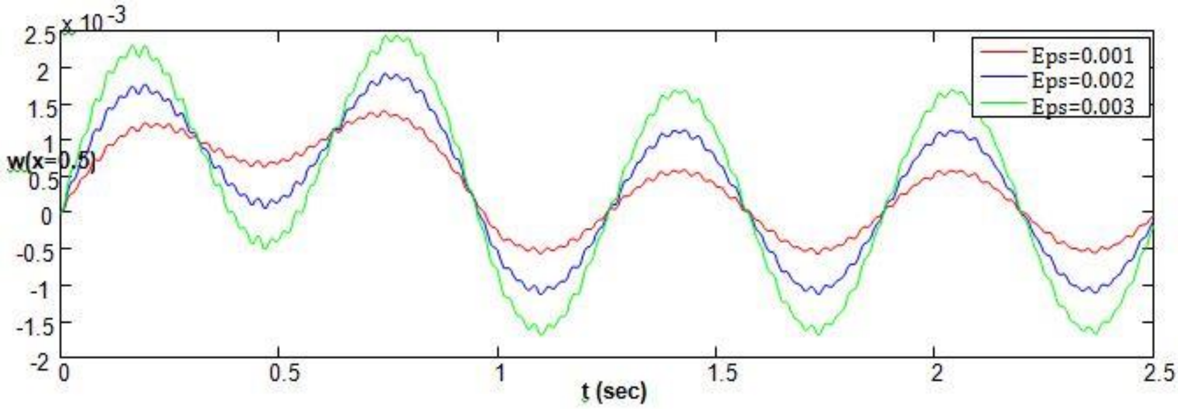

Fig. 9. Vibration of a poroelastic beam with an attached mass-spring system and a non-ideal support subjected to a moving load ($\varepsilon_1 = \varepsilon_2 = Eps$)

5. Conclusions

The novelties of the present approach may be summarized as follows:

1. Dynamic analysis of poroelastic beams with moving loads was performed for the first time.
2. The complexity increases by considering non-ideal supports and attached mass-spring systems.
3. Free and forced vibration responses of Euler-Bernoulli and Timoshenko elastic beams were compared with those of poroelastic beams.
4. The governing-coupled PDE equations of the forced vibration of the saturated poroelastic beam were analytically solved by using Laplace and finite Fourier transforms.

Apart from the novelties presented in the modeling and solution stages, some of the practical conclusions of this study can be summarized as follows:

1. The poroelasticity nature of the material properties attenuates the vibration amplitude and leads to structural damping.
2. Due to the occurrence of anti-phase vibration modes, increasing the magnitude of the attached mass may lead to grown amplitudes of vibration for beams with moving loads. However, the natural frequency of a beam may not be considerably affected by the magnitude of the suspended mass (unless a considerably heavy mass is used).
3. The vibration pattern may be changed from a global one with superimposed local oscillations to a disordered local or beat-type by selecting a proper magnitude of the attached mass.
4. Since amplitude of the superimposed transient vibrations of a beam with non-ideal support experiences small changes with the amplitude of the support excitation, the total amplitude of the vibration does not vary in proportion to the amplitude of the support excitations.
5. The amplitude of the vibration of the beam is generally not proportional to the magnitude of a moving load and the moving speed only slightly affects the vibration amplitude. Moreover, when a load passes over a poroelastic beam, the amplitude of the vibration at the moment of leaving the beam becomes greater at higher passage speeds.

References

[1].Wong J.Y., 2001, *Theory of ground vehicles*, John Wiley & Sons Inc, New York, Third Edition.

[2].Jazar R.N., 2008, *Vehicle Dynamics: Theory and Applications*, Springer.

[3].Ellis B.R., Ji T., 1997, Human–structure interaction in vertical vibrations, In: *Proceedings of the Institution of Civil Engineers—Structures and Buildings* 122(1): 1–9.

[4].Snowdon J.C., 1966,Vibration of cantilever beams to which dynamic absorbers are attached, *Journal of Acoustic Society of America* 39: 878.

[5].Lee H.P.,1996, Dynamic response of a beam with a moving mass, *Journal of Sound and Vibration* 191: 289-294.

[6].Mofid M., Tehranchi A., Ostadhossein A., 2010, On the viscoelastic beam subjected to moving mass, *Advance in Engineering Software* 41(2): 240-247.

[7].Bulut H., Kelesoglu O., 2010, Comparing numerical methods for response of beams with moving mass, *Advances in Engineering Software* 41(7-8): 976-980.

[8].Garinei A., 2006, Vibrations of simple beam-like modelled bridge under harmonic moving loads, *International Journal of Engineering Science* 44(11-12):778-787.

[9].Şimşek M., Kocatürk T., 2009, Free and forced vibration of a functionally graded beam subjected to a concentrated moving harmonic load, *Composite Structures* 90(4): 465-473.

[10]. Raftoyiannis I.G., Avraam T.P., Michaltsos G.T., 2014, Analytical models of floating bridges under moving loads, *Engineering Structures* 68(1): 144-154.

[11]. Şimşek M., 2010, Non-linear vibration analysis of a functionally graded Timoshenko beam under action of a moving harmonic load, *Composite Structures* 92(10): 2532-2546.

[12]. Wang Y.-M., Chen C.-H., 2012, The transient dynamics of a moving mass traveling on an eccentric path along a finite simple supported inextensible beam, *International Journal of Mechanical Sciences* 55(1): 118-128.

[13]. Turhan O., 2000, On the fundamental frequency of beams carrying a point mass: Rayleigh approximation versus exact solutions, *Journal of Sound and Vibration* 230(2): 449-459.

[14]. Chiba M., Sugimoto T.,2003, Vibration characteristics of a cantilever plate with attached spring–mass system, *Journal of Sound and Vibration* 260(2):237–263.

[15]. Zhang D., CowinS.C., Oscillatory bending of a poroelastic beam, *Journal of Mechanics and Physics of Solids*42(10): 1575–1599.

[16]. Wang Z.H., Prevost J.H., Coussy O., 2009, Bending of fluid-saturated poroelastic beams with compressible constitutes, *International Journalfor Numericaland AnalyticalMethods in Geomechanics* 33(4): 425–447.

[17]. Li L.P., Schulgasser K., Cederbaum G., 1998, Large deflection analysis of poroelastic beams, *International Journal of Non-Linear Mechanics* 33(1): 1-14.

[18]. Biot M.A., 1941, General theory of three-dimensional consolidation, *Journal of Applied Physics* 12: 155–164.

[19]. Cederbaum G., Li L., Schulgasser K., 2000, *Poroelastic structures*, Elsevier Science Ltd., Oxford, UK.

[20]. de Boer R., 2003, Reflections on the development of the theory of porous media, *AppliedMechanics Reviews* 56(6): 27–42.

[21]. Schrefler B.A., 2002, Mechanics and thermodynamics of saturated/unsaturated porous materials and quantitative solution, *Applied Mechanics Reviews* 55(4): 351–388.

[22]. Yang X., Li L., 2006, Mathematical model for dynamics of incompressible saturated poroelastic beam and rod (in Chinese), *Acta Mech Solida Sinica* 27: 159–166.

[23]. Yang X., Wen Q., 2010, Dynamic and quasi-static bending of saturated poroelastic Timoshenko cantilever beam, *Applied Mathematics and Mechanics*-English Edition 31(8): 995–1008.

[24]. Yi Y., Li L., Xiao Y., 2009, Quasi-static and dynamical bending of a cantilever poroelastic beam, Journal of Shanghai University (English Ed) 13(3): 189–196.

[25]. Niskos D., Theodorakopoulos D., 1994, Flexural vibrations of poroelastic plate, *Acta Mechanica* 103: 191–203.

[26]. Busse A., Schanz M., Antes B., 2003, A poroelastic Mindlin-plate, *Proceedings in Applied Mathematics and Mechanics*3(1):260–261.

[27]. Yang S.S.G.Y.X., 2010, Mathematical model for dynamic of incompressible saturated poroelastic Timoshenko beam, Chinese Journal of Solid Mechanics 2010-4.

[28]. Pakdemirli M., Boyaci H., 2002, Effect of non-ideal boundary conditions on the vibrations of continuous systems, *Journal of Sound and Vibration* 249(4): 815–823.

[29]. Pakdemirli M., Boyaci H., 2003, Non-linear vibrations of a simple–simple beam with a non-ideal support in between, *Journal of Sound and Vibration* 268(2): 331–341.

[30]. Aydogdu M., Ece M.C., 2006, Buckling and vibration of non-ideal simply supported rectangular isotropic plates, *Mechanics Research Communication* 33(4):532–540.

[31]. Malekzadeh K., Khalili S.M.R., Abbaspour P., 2010, Vibration of non-ideal simply supported laminated plate on an elastic foundation subjected to in-plane stresses, *Composite Structures* 92(6): 1478–1484.

[32]. Boyacı H., 2007, Beam vibrations with non-ideal boundary conditions, *Springer Proceedings in Physics* 111: 97-102.

[33]. Eigoli A.K., Ahmadian M.T., 2011, Nonlinear vibration of beams under nonideal boundary conditions, *Acta Mechanica* 218(3-4): 259-267.

[34]. Zarfam R., Khaloo A.R., Nikkhoo A., 2013, On the response spectrum of Euler–Bernoulli beams with a moving mass and horizontal support excitation, *Mechanics Research Communication* 47 :77-83.

[35]. Rao S., 2010, *Mechanical vibrations*, Prentice Hall, Fifth Edition.

[36]. Sneddon I.N., 1972, *The use of integral transforms*, McGraw-Hill.

[37]. Fryba L., 1999, *Vibration of solids and structures under moving loads*, Groningen. Thomas Telford Ltd., London, Third Edition.